University of Lethbridge Research Repository

OPUS

http://opus.uleth.ca

Faculty Research & Publications

Das, Saurya

2015-12-15

Multiple kinetic k-essence, phantom barrier crossing and stability

Sur, Sourav

http://hdl.handle.net/10133/3829

Multiple kinetic k-essence, phantom barrier crossing and stability

Sourav Sur and Saurya Das

Dept. of Physics, University of Lethbridge
4401 University Drive, Lethbridge, Alberta, Canada T1K 3M4

E-mail: sourav.sur@uleth.ca and saurya.das@uleth.ca

Abstract. We investigate models of dark energy with purely kinetic multiple k-essence sources that allow for the crossing of the phantom divide line, without violating the conditions of stability. It is known that with more than one kinetic k-field one can possibly construct dark energy models whose equation of state parameter w_x crosses -1 (the phantom barrier) at recent red-shifts, as indicated by the Supernova Ia and other observational probes. However, such models may suffer from cosmological instabilities, as the effective speed of propagation c_x of the dark energy density perturbations may become *imaginary* while the $w_x = -1$ barrier is crossed. Working out the expression for c_x we show that multiple kinetic k-essence fields do indeed lead to a $w_x = -1$ crossing dark energy model, satisfying the stability criterion $c_x^2 \geq 0$ as well as the condition $c_x \leq 1$ (in natural units), which implies that the dark energy is not super-luminal. As a specific example, we construct a phantom barrier crossing model involving three k-fields for which c_x is a constant, lying between 0 and 1. The model fits well with the latest Supernova Ia Union data, and the best fit shows that w_x crosses -1 at red-shift $z \sim 0.2$, whereas the dark energy density nearly tracks the matter density at higher red-shifts.

1. Introduction

The late-time accelerated expansion of the universe is now well established through the observations of the luminosity distance – red-shift relation for type Ia Supernovae (SNIa) [1, 2, 3, 4, 5, 6, 7, 8]. Measurements of the cosmic microwave background (CMB) temperature fluctuations by the Wilkinson Microwave Anisotropy Probe (WMAP) [9, 10] as well as the large scale red-shift data from the Sloan Digital Sky Survey (SDSS) [11] further indicate that the universe is very nearly spatially flat and consists of about 70% of dark energy (DE) which drives the cosmic acceleration. The value of the DE equation of state (EoS) parameter, i.e., the ratio of pressure to energy density of DE, $w_X = p_X/\rho_X$, should be less than $-1/3$ to maintain this acceleration. Although the simplest candidate for DE is a cosmological constant (Λ), for which $w_X = -1$, there are serious theoretical problems associated with it [12]. Λ needs to be extremely *fine tuned* so that the DE at present is small compared to the Planck scale. A fine tuning is also required to keep the (Λ-) dark energy density ρ_X comparable with the present critical density ρ_{0c}, while the acceleration begins only in the recent past — the *coincidence problem*. From the observational point of view, although there are indications that w_X is very close to -1 at present, combined studies of SNIa, CMB and baryon acoustic oscillation (BAO) peaks do actually point toward a *dynamical* DE with EoS parameter w_X slowly varying with red-shift z. More specifically, the so-called ΛCDM model, which consists of Λ and cold dark matter as dominant components, although consistent with the low-z observational data, does not produce sufficiently good fits with the data at relatively higher z ($\gtrsim 1$). Accordingly, there have been a large number of model-independent and model-dependent DE parameterizations explored in the literature [13, 14, 15, 16, 17]. Extensive studies reveal that in parameterizing the DE to produce good fits with the observational data, it is always desirable to have no inherent restriction imposed on w_X from the underlying theory. For instance, it is not desirable to have w_X always ≥ -1, which is required for the theoretical consistency of many popular DE models, such as quintessence, tachyon, dilaton, etc. For the reviews on various dynamical aspects of DE, see [18].

Within the scope of minimally coupled canonical scalar field DE models, such as quintessence [19], the crossing from $w_X > -1$ to $w_X < -1$ can never happen and there is a need of more than one scalar field, at least one of which is of *phantom* nature, i.e., carries a wrong sign in front of the kinetic term [20]. For this reason the $w_X = -1$ line is commonly known as the phantom divide line (PDL). Phantom fields violate the dominant energy condition, and therefore could give rise to classical instabilities [21]. Moreover, since the phantom energy density is unbounded from below, the quantum mechanical stability is in jeopardy. The vacuum is unstable against the decay into ghosts and positive energy particles, which couple to gravitons producing further decay into cosmic gamma rays [22]. In an expanding Friedmann universe, the extremely repulsive (anti-gravitating) nature of the phantom fields pose more problems as the phantom energy density generically tends to infinity in finite time in future leading to the so-

called "Big Rip" singularity [23], as well as some other mild singularities. For a general categorization of these singularities see for instance [24].

Apart from the coupled quintessence and phantom models, commonly known as the *quintom* models [25], there are various other models in which the phantom barrier crossing is shown to be achieved in a consistent way. Notable among these are the scalar-tensor models [26], brane-world models [27], string-inspired dilatonic ghost condensate models [28], quantum-corrected Klein-Gordon models with quartic potential [29], coupled DE models [30], modified gravity models [31], H-essence (complex scalar) models [32], etc. In this work, we focus on the so-called k-essence models [33, 34], which incorporate a natural generalization of quintessence via a Lagrangian with non-linear dependence on the kinetic term(s) for the scalar field(s). For such models w_x is not constrained to be ≥ -1 and may in principle cross the PDL. However, it has been argued by Vikman [35] that in the case of a single field k-essence model, with a Lagrangian of the form $P(\phi, X)$, where $X = -\frac{1}{2}[\nabla\phi]^2$ is the kinetic term of the scalar field ϕ, the PDL crossing either leads to instabilities against cosmological perturbations or is realized by a discrete set of phase space trajectories‡. For a multiple k-essence model, involving more than one k-fields ϕ_I ($I = 0, \ldots, N-1$), with kinetic terms $X_I = -\frac{1}{2}[\nabla\phi_I]^2$, the PDL crossing is shown to be possible even when the Lagrangian is purely a function of the kinetic terms, $P = \sum P_I(X_I)$ [38]. However, the stability of such a model against cosmological perturbations have not been explored in the literature.

A major difficulty in dealing with the equations of scalar-type cosmological perturbations for multiple scalar fields is that these equations are extremely coupled in the curvature and isocurvature modes, even when the scalar fields are only minimally coupled to gravity [39, 40, 41, 42]. For multiple k-essence, the perturbation equations are complicated further, however there are some specific cases in which the expression for the speed of propagation c_x of the curvature perturbations could be obtained and the stability analysis could be performed [43, 44]. For example, when the k-essence Lagrangian is $P(\mathbf{\Phi}, X)$, where $\mathbf{\Phi} = (\phi_0, \phi_1, \cdots)$ and $X = -\frac{1}{2}\mathcal{G}^{IJ}(\mathbf{\Phi})\nabla_\mu\phi_I\nabla^\mu\phi_J$ [43], the propagation speed is simply given by the well-known result of Garriga and Mukhanov [45], i.e., $c_x^2 = \frac{\partial P}{\partial X}/\frac{\partial\rho_X}{\partial X}$. On the other hand, in the multi-field Dirac-Born-Infeld (DBI) inflationary scenario, the propagation speed for the Lagrangian $P = -f^{-1}(\mathbf{\Phi})\sqrt{1 - 2Xf(\mathbf{\Phi})} - V(\mathbf{\Phi})$, is given in a homogeneous background by $c_x = \sqrt{1 - 2Xf(\mathbf{\Phi})}$ [44]. However, none of these expressions for c_x will hold for the most general Lagrangian $P = \sum P_I(\phi_I, X_I)$, corresponding to the N non-interacting fields $\mathbf{\Phi} = (\phi_0, \phi_1, \cdots)$. A comprehensive study of the curvature perturbation equations reveals that one can, in principle, obtain the expression of c_x for the multi k-field Lagrangian $P = \sum P_I(\phi_I, X_I)$ [46], leaving aside the isocurvature modes which couple weakly with the curvature mode in the large-scale limit [40, 41].

In this paper we first investigate whether the multiple kinetic k-essence DE models

---

‡ There are however some counter-arguments and counter-examples set in [36, 37] and it is shown that for a generalized single field k-essence Lagrangian of the form $P(\phi, X) = f(\phi)X - V(\phi)$ stable PDL crossing is indeed possible for some specific functional form of $f(\phi)$ and $V(\phi)$.

that allow the PDL crossing is cosmologically *stable*, i.e., the speed of propagation c_X of the DE density perturbations satisfies the condition $c_X^2 \geq 0$. It is also relevant to check whether $c_X \leq 1$ (in natural units), so that the DE perturbations do not travel faster than light [47]. However, the requirement $c_X \leq 1$ is not potentially stringent, because it has been argued that causal paradoxes do not necessarily arise even when $c_X > 1$ [48]. We find that in most circumstances (including the model described in [38]) where c_X dynamically varies with time, the PDL crossing is associated with a flip of sign of c_X^2, thus giving rise to violent instability. An appropriate choice for c_X^2 in a stable DE model is therefore a *constant* whose value lies between 0 and 1. Imposing this condition on c_X^2 we work out the constraint on the field configuration. As a specific example we try to construct a stable PDL crossing DE model using this constraint and with the least number of model parameters possible, so as to determine these parameters with less uncertainties by fitting with the observational data. While within the scope of two k-fields the stability constraint leads to complicated field solutions, we construct a reasonably simpler model involving three k-fields for which stable PDL crossing is possible.

We constrain the parameters of the model using the most recent data-set released by the Supernova Cosmology Project (SCP) team [7], viz., the "Union" compilation, which consists of 414 SNIa reduced to 307 usable data points after various selection cuts. Marginalizing over the Hubble constant H_0, we find that the best fit value of the present matter density parameter $\Omega_{0m} \simeq 0.265$, whereas the best fit DE EoS parameter w_X crosses the PDL at red-shift $z = z_c \sim 0.2$, fairly in agreement with z_c found in many model-independent DE parameterizations [49]. The minimized value of the χ^2 statistic is found to be about 310.4, which shows an improvement of $\Delta \chi^2 \sim -2.7$ over the minimized χ^2 for the ΛCDM model found with the Union data-set [8]. The minimized χ^2 per degree of freedom for the model discussed in this paper is 1.011, which is also marginally better than that found in [6] for the ΛCDM model using the older SNIa data-set complied by Riess *et al* [4]. Additionally, we see that the best fit value of the DE density almost tracks the matter density over sufficiently longer red-shift range in the past until becoming dominant after $z \simeq 0.4$. Thus the model provides a possible resolution of the coincidence problem. Extrapolation of the best fit w_X to future epochs shows a tendency of w_X to turn back towards -1 after reaching a minimum value. Thus the phantom regime appears to be transient and future singularities, such as the Big Rip, may be avoided.

The present model also differs from the usual quintom model [25] implemented using two (or possibly more) scalar fields, (at least) one of which has a negative definite kinetic energy density (i.e., phantom), and as such the EoS parameter is less than -1, whereas the other field(s) has(have) positive definite kinetic energy (quintessence-type) and EoS parameter(s) greater than -1. The negative energy field comes to dominate at late times and is responsible for the PDL crossing. In the three-field k-essence model which we study, two of the k-fields have positive definite energy density, whereas the energy density of the third k-field is negative for a sufficiently longer time in the past

and present, but may become positive in distant future, as found by extrapolating the best fit model parameters to future (negative) red-shifts. In that sense the third k-field may not be regarded as equivalent to an eternal phantom, and quantum mechanical instabilities may be avoided. None of the fields have EoS parameter less than -1, unlike quintom models. Moreover, the negative energy k-field is not responsible for the super-acceleration ($w_X < -1$), it is a positive energy k-field that causes the PDL crossing, again in contrast with what happens in quintom models.

This paper is organized as follows: in sec. 2 we describe the general framework of multiple k-essence DE models assuming that there are no mutual interactions between the individual k-fields. In sec. 3 we consider the simplistic case of purely kinetic multiple k-essence and show that only for more than one dynamical k-fields the PDL crossing is possible, although the field configuration is severely constrained by the stability criterion. We work out this constraint and choose the value of the speed of propagation c_X of the DE density perturbations to be a constant, in order to have a stable PDL crossing multiple kinetic k-essence DE model. In sec. 4 we construct a specific multiple k-field model for which c_X is constant, and w_X crosses the PDL in recent past. In sec. 5 we fit this model with the 307 Union SNIa data [7], to reconstruct phenomenologically the multiple k-essence Lagrangian. We conclude with a summary and open questions in sec. 6. In the Appendix, we work out the equations of scalar-type cosmological perturbations for a multiple k-essence field configuration so as to find the expression for the propagation speed c_X.

2. General Formalism

Let us consider the following action in $(3 + 1)$ dimensions:

$$S = \int d^4x \sqrt{-g} \left[\frac{R}{2\kappa^2} + P(\mathbf{\Phi}, \mathbf{X}) + \mathcal{L}_m \right] , \quad P(\mathbf{\Phi}, \mathbf{X}) = \sum_{I=0}^{N-1} P_I(\phi_I, X_I) , \tag{1}$$

where $\kappa^2 = 8\pi G$ is the gravitational coupling constant, $\mathcal{L}_m$ is the Lagrangian density for perfect fluid matter, $\mathbf{\Phi} = (\phi_0, \cdots, \phi_{N-1})$ are a set of N mutually non-interacting scalar fields, and $\mathbf{X} = (X_0, \cdots, X_{N-1})$ where X_I stands for the kinetic term of the scalar field ϕ_I:

$$X_I = -\frac{1}{2} g^{\mu\nu} \partial_\mu \phi_I \partial_\nu \phi_I \quad , \qquad (\text{no sum over } I = 0, \cdots, N-1) . \tag{2}$$

$P_I(\phi_I, X_I)$ is the k-essence Lagrangian density for the field ϕ_I.

We assume the space-time structure to be described by a spatially flat Robertson-Walker (RW) line-element

$$ds^2 = -dt^2 + a^2(t) \left[dr^2 + r^2 \left(d\vartheta^2 + \sin^2 \vartheta d\varphi^2 \right) \right] \tag{3}$$

where $a(t)$ is the scale factor which is normalized to unity at the present epoch $t = t_0$. In such a space-time, the kinetic term reduces to $X_I = \dot{\phi}_I^2/2$, where the over-dot stands

for d/dt. The field equations are the Friedmann equations given by

$$H^2 \equiv \left(\frac{\dot{a}}{a}\right)^2 = \frac{\kappa^2}{3}\left(\rho_m + \rho_X\right) \quad , \qquad \dot{H} \equiv \frac{\ddot{a}}{a} - \frac{\dot{a}^2}{a^2} = -\frac{\kappa^2}{2}\left[\rho_m + \rho_X + p_m + p_X\right] , \qquad (4)$$

where $H = \dot{a}/a$ is the Hubble expansion rate, ρ_m and p_m are the perfect fluid energy density and pressure respectively, ρ_X and p_X are the k-essence energy density and pressure respectively, given by

$$\rho_X = \sum_{I=0}^{N-1} \rho_I(\phi_I, X_I) = \sum_{I=0}^{N-1}\left(2X_I\frac{\partial P_I}{\partial X_I} - P_I\right) \quad , \qquad p_X = \sum_{I=0}^{N-1} P_I(\phi_I, X_I). \quad (5)$$

Considering the perfect fluid matter in the form of pressure-less dust ($p_m = 0$), the field equations integrate to give the matter energy density as $\rho_m = \rho_{0m}/a^3$, where ρ_{0m} is the present value of ρ_m. From Eq.(4) one obtains the expression for the normalized Hubble rate:

$$\tilde{H} \equiv \frac{H}{H_0} = \left[\frac{\rho_X}{\rho_{0c}} + \frac{\Omega_{0m}}{a^3}\right]^{1/2} , \qquad (6)$$

where H_0 is the present value of the Hubble parameter H and $\rho_{0c} = 3H_0^2/\kappa^2$, $\Omega_{0m} = \rho_{0m}/\rho_{0c}$ are the present values of the critical density and matter density parameter respectively.

The equations of motion of the scalar fields $\mathbf{\Phi} = (\phi_0, \cdots, \phi_{N-1})$ are given as

$$\frac{d}{dt}\left(a^3\dot{\phi}_I\frac{\partial P_I}{\partial X_I}\right) = a^3\frac{\partial P_I}{\partial \phi_I} \qquad \text{(for all } I), \qquad (7)$$

and the mutually non-interacting individual field components satisfy the continuity equation:

$$\dot{\rho}_I = 3H\left(1 + w_I\right)P_I \qquad \text{(for all } I), \qquad (8)$$

where $w_I = P_I/\rho_I$ are the EoS parameters for the individual fields ϕ_I. The EoS parameter w_X for the k-essence DE is thus given by

$$w_X = \frac{p_X}{\rho_X} = \sum_{I=0}^{N-1}\frac{w_I\rho_I}{\rho_X} = -1 - \frac{\dot{\rho}_X}{3H\rho_X}. \qquad (9)$$

Using Eqs. (4) and (6) one can express the total EOS parameter w in terms of w_X:

$$w = \frac{p_X}{\rho_m + \rho_X} = w_X\left(1 - \frac{\Omega_{0m}}{\tilde{H}^2 a^3}\right). \qquad (10)$$

The deceleration parameter q is given by

$$q = -\frac{\ddot{a}}{aH^2} = \frac{1 + 3w}{2}. \qquad (11)$$

For an accelerated expansion of the universe ($q < 0$) the total EOS parameter w should be less than $-1/3$, and as can be observed from Eq. (10), w_X is further less than $-1/3$. Although the observations favour the value of w_X to be very close to that for a cosmological constant (i.e., -1) at present and in recent past, extensive studies show that better fits with observational data require a dynamical DE with w_X substantially

greater than -1 at relatively higher red-shifts ($z = a^{-1} - 1 \gtrsim 1$). Moreover, for consistent statistical data fits it is not desirable to always have a theoretical restriction such as $w_X \geq -1$. In other words, the dynamical DE models that allow the PDL crossing are most suited for analyzing the observational data so as to determine the cosmic evolution history over the entire red-shift range that is probed. While such a crossing in minimally coupled scalar field DE models is associated with violent cosmological instabilities, one has to ensure that the instabilities never occur in the multiple k-essence DE models. For such models the expression of the square of the speed of propagation of curvature perturbations is found to be (see the Appendix for detailed derivation)

$$c_X^2 = (\rho_X + p_X) \left[\sum_{I=0}^{N-1} \frac{\rho_I + P_I}{\tilde{c}_I^2} \right]^{-1} , \qquad \text{where} \quad \tilde{c}_I^2 = \frac{\partial P_I / \partial X_I}{\partial \rho_I / \partial X_I} . \tag{12}$$

In the case of a single k-field ($I = 0$, say) the above Eq. (12) reduces to the well-known result $c_X^2 = \tilde{c}_0^2 = \frac{\partial P_0}{\partial X_0} / \frac{\partial \rho_0}{\partial X_0}$ [45]. The value of c_X^2 must be non-negative, for the stability of a model, and always be less than unity (in natural units) so that the DE perturbations do not travel faster than light.

In the next section we examine the plausibility of a stable PDL crossing in the multiple k-essence scenario, considering for simplicity the k-field Lagrangian to be purely kinetic in nature.

3. Purely kinetic multiple k-essence

When the k-essence Lagrangian is purely a function of the kinetic terms $\mathbf{X} = (X_0, \cdots, X_{N-1})$, i.e., $P_I = P_I(X_I)$, ($I = 0 \cdots, N-1$), the equations of motion (7) for the scalar fields $\mathbf{\Phi} = (\phi_0, \cdots, \phi_{N-1})$ can be integrated at once to give

$$a^3 \dot{\phi}_I \frac{dP_I}{dX_I} = \text{constant} \quad (k_I) , \qquad \text{for all } I . \tag{13}$$

However, remembering that $X_I = \dot{\phi}_I^2 / 2$ in Robertson-Walker space-time, one may observe that the expressions (5), (9) and (12), for ρ_X, w_X and c_X^2 respectively, remain invariant under a field redefinition $\phi_I \rightarrow k_I \phi_I$. Hence the constants k_I can effectively be set to unity, for all I, and the above equation can be rewritten as

$$\sqrt{2X_I} \frac{dP_I}{dX_I} = \frac{1}{a^3} , \qquad \text{for all } I . \tag{14}$$

Now, using the definitions (5) of ρ_X and ρ_I, we can express the DE EoS parameter w_X, Eq. (9), and the square of the propagation speed of perturbations c_X^2, Eq. (12), as

$$w_X = -1 + \frac{1}{\rho_X} \sum_{I=0}^{N-1} 2X_I \frac{dP_I}{dX_I} , \quad c_X^2 = \frac{\sum_{I=0}^{N-1} 2X_I dP_I / dX_I}{\sum_{I=0}^{N-1} \left[2X_I dP_I / dX_I + 4X_I^2 d^2 P_I / dX_I^2 \right]} . \tag{15}$$

For a transition from $w_X > -1$ to $w_X < -1$, the quantity $\sum 2X_I dP_I / dX_I$ needs to vanish at the PDL cross-over scale factor $a = a_c$.

In the case of a single scalar field $\phi_I = \phi_0$, say, and $P_I(X_I) = P_0(X_0)$, the PDL crossing implies that $X_0 (dP_0 / dX_0)|_{a=a_c} = 0$, i.e., either $X_0(a = a_c)$ or $dP_0 / dX_0|_{a=a_c}$ or

both must vanish. This is clearly not possible for any finite value of a since from Eq.(14) we have $\sqrt{2X_0}(dP_0/dX_0) = a^{-3}$.

For more than one k-fields the PDL crossing is in principle possible whenever the quantity $\sum 2X_I(dP_I/dX_I) = 0$ at $a = a_c$, i.e., $\sum \sqrt{2X_I}\big|_{a=a_c} = 0$, by Eq. (14). However, from Eq. (15) we find that the change of sign of $\sum 2X_I(dP_I/dX_I)$ as the $w_X = -1$ line is crossed, implies a change of sign of sign of c_X^2 as well, unless the numerator and denominator of c_X^2 exactly cancel each other to give a value which never flips sign. For example, if P_I is a function of some numerical power of X_I, i.e., $P_I = X_I^{\nu_I}$ (for all I), as has been considered in ref. [38], there is always a flip of sign of c_X^2 associated with the PDL crossing. Therefore unless one chooses c_X^2 to be such a function of a which does not change sign for any value of a, instabilities are bound to be there even in multiple k-essence DE models. Moreover, we must have $c_X^2 \leq 1$ in order that the DE perturbations do not travel faster than light. The simplest possible choice of c_X^2, appropriate for a stable and non-super-luminal DE model is

$$c_X^2 = n \text{ (constant)} \quad , \qquad 0 \leq n \leq 1 . \tag{16}$$

Of course, the limiting case $n = 0$ implies a non-propagating DE (for example, due to a cosmological constant). For dynamic DE models we have $0 < n \leq 1$.

Let us now denote

$$y_I = \sqrt{2X_I} = \dot{\phi}_I \text{ in RW space-time} . \tag{17}$$

Eq. (14) reduces to

$$\frac{dP_I}{dy_I} = \frac{1}{a^3} \qquad \text{for all } I , \tag{18}$$

and the DE energy density takes the form

$$\rho_X = \sum_{I=0}^{N-1} \rho_I \quad , \qquad \rho_I = \frac{y_I}{a^3} - P_I . \tag{19}$$

From these equations we find

$$y_I(a) = -\frac{a^4 \rho_I'(a)}{3} \qquad \text{for all } I . \tag{20}$$

where prime $\{'\}$ denotes d/da. Eqs. (15) for w_X and c_X^2 reduce to

$$w_X = -1 + \frac{y(a)}{a^3 \rho_X} \quad , \qquad c_X^2 = -\frac{ay(a)}{3}\left[\sum_{I=0}^{N-1} y_I^2/y_I'\right]^{-1} , \qquad \text{where } y(a) = \sum_{I=0}^{N-1} y_I(a) . \tag{21}$$

We rewrite the expression for c_X^2 in the form

$$3\, c_X^2 \frac{y_I^2}{y_I'} + ay_I(a) = -\eta_I(a) , \tag{22}$$

where the arbitrary functions $\eta_I(a)$ satisfy the relation $\sum \eta_I(a) = 0$. With the choice $c_X^2 = n$ (constant), we therefore have

$$\frac{y_I'}{y_I}\left[1 + \frac{\eta_I(a)}{ay_I(a)}\right] = -\frac{3n}{a} \quad , \qquad \sum_{I=0}^{N-1} \eta_I(a) = 0 . \tag{23}$$

While from Eq. (21) we see that the PDL crossing requires $y = \sum y_I = 0$ at $a = a_c$, a stable k-field configuration is the one that solves the above equation (23). In the next section we construct a cosmologically stable PDL crossing DE model by suitably choosing a specific field configuration and a reasonably simplified ansatz to solve for y, w_X and ρ_X. We fit the solutions to the latest SNIa Union data [7] in the subsequent section, show the plausible tracking of the dark energy density to the matter density in the past, avoidance of future singularities, and finally reconstruct the multiple kinetic k-essence Lagrangian.

4. Cosmologically stable PDL crossing multiple kinetic k-essence model

4.1. Two k-field configuration

Let us first consider a field configuration involving only two scalar fields:

$$ I = 0, 1 \quad ; \qquad \mathbf{\Phi} = (\phi_0, \phi_1) \quad ; \qquad \eta_0(a) = -\eta_1(a) = \eta(a) \, , \quad \text{say} \, . \tag{24} $$

From Eq. (23) we have

$$ \frac{y_0'}{y_0} \left(1 + \frac{\eta}{ay_0} \right) = \frac{y_1'}{y_1} \left(1 - \frac{\eta}{ay_1} \right) = -\frac{3n}{a} \, . \tag{25} $$

Let us assume a power-law solution for y_1 as

$$ y_1 = \alpha_1 \, a^s \quad , \qquad \alpha_1, s = \text{constants} \, . \tag{26} $$

Plugging this in Eq. (20) and integrating, and using Eq. (19), we get the expressions for the energy density and the pressure corresponding to the field ϕ_1 as

$$ \rho_1 = \begin{cases} \left(\frac{3}{3-s} \right) \alpha_1 a^{s-3} + \lambda_1 & (s \neq 3) \\ -3\alpha_1 \ln a + \lambda_1 & (s = 3) \end{cases} \, , \quad P_1 = \begin{cases} -\left(\frac{s}{3-s} \right) \alpha_1 a^{s-3} - \lambda_1 & (s \neq 3) \\ \alpha_1 a^{s-3} - 3\alpha_1 \ln a - \lambda_1 & (s = 3) \end{cases} \tag{27} $$

where λ_1 is a constant.

Substituting Eq. (26) in Eq. (25) and eliminating $\eta(a)$ we obtain

$$ \left(1 + \frac{s}{3n} \right) \frac{y_0'}{y_0} = \frac{(1 + y_0/y_1)'}{1 + y_0/y_1} \, . \tag{28} $$

Integrating this we get the algebraic equation

$$ y_0 + y_1 \left(1 - C y_0^{1+s/3n} \right) = 0 \, , \tag{29} $$

where C is an integration constant.

We look for the simplest possible solutions of the above equation (29), so that the cosmological quantities ρ_X and w_X (and hence the normalized Hubble expansion rate $\tilde{H}$) have reasonably simple forms which we can fit with the observational data.

Let us first take into account the cases $s = -3n$ or $s = 0$ for either of which Eq. (29) is linear in y_2. However, for $s = -3n$, Eq. (29) gives $y_0 \propto y_1$, i.e., $y = y_0 + y_1 \propto a^{-3n}$, which can never change sign for any finite value of a. Therefore we rule out $s = -3n$ as a possible choice for a PDL crossing DE model. For $s = 0$, on the other hand, we obtain from Eqs. (26) and (29) that $y_0 = y_1/(Cy_1 - 1) = \text{constant}$, i.e., the corresponding fields

ϕ_1 and ϕ_2 are non-dynamical, and PDL crossing never happens either. Hence we rule out the choice $s = 0$ as well.

We next consider the case $s = 3n/2$ for which Eq. (29) is quadratic in y_0. Corresponding to $0 \leq n \leq 1$, we have $0 \leq s \leq 3$. The solution of Eq. (29) is given by

$$y_0 = \alpha_0\, a^{-s} \left[1 \pm \sqrt{1 + \frac{2\alpha_1 a^{2s}}{\alpha_0}} \right], \tag{30}$$

where we denote $\alpha_0 = 1/(2C\alpha_1)$. From Eqs. (26) and (30) we see once again that the expression for $y = y_0 + y_1$ cannot change sign, i.e., the PDL crossing is not possible.

We are therefore left with the choices of the parameter s which render Eq. (29) to be cubic, quartic or even higher order algebraic equation in y_0§. The solutions for y_0 are however very complicated and leads to messy expressions for the corresponding energy density. An inspection of Eq. (29) also reveals that the choices of s for which Eq. (29) is even order (quadratic, quartic, etc.) in y_0, can be ruled out anyway, because $y = y_0 + y_1 = Cy_1 y_0^{1+s/3n}$ can in no way change sign when the power $(1 + s/3n)$ is an even integer. In a separate work which is in progress [50] we examine the cases for which Eq. (29) is cubic or higher order in y_0. In the present paper, however, we choose to work with a simpler alternative by introducing one more k-field, in a way that Eq. (29) remains quadratic in y_0, and the above solution (30) could be used.

4.2. Three k-field configuration

Let us now consider the following configuration that involves three scalar fields:

$$I = 0, 1, 2 \quad ; \qquad \mathbf{\Phi} = (\phi_0, \phi_1, \phi_2) \quad ; \qquad \eta_0(a) = -\eta_1(a) = \eta(a), \quad \eta_2 = 0. \tag{31}$$

From Eq. (23) we have

$$\frac{y_0'}{y_0}\left(1 + \frac{\eta}{ay_0}\right) = \frac{y_1'}{y_1}\left(1 - \frac{\eta}{ay_1}\right) = \frac{y_2'}{y_2} = -\frac{3n}{a}. \tag{32}$$

The solution for y_2 is

$$y_2 = \alpha_2\, a^{-3n} \quad , \qquad \alpha_2 = \text{constant}. \tag{33}$$

whence from Eqs. (19) and (20) we find the energy density and the pressure corresponding to the field ϕ_2 as

$$\rho_2 = \frac{\alpha_2}{n+1} a^{-3(n+1)} + \lambda_2 \quad , \qquad P_2 = \frac{n\alpha_2}{n+1} a^{-3(n+1)} - \lambda_2, \tag{34}$$

where λ_2 is a constant.

Once again, we assume the power-law solution (26) for y_1, so that the energy density and the pressure corresponding to the field ϕ_1 are given by (27), and y_0 is related to y_1 through the relation (29). Similar to the case of two k-fields, it is easy to show that the PDL crossing never happens for three k-fields as well, if the parameter $s = -3n$ or 0

---

§ There are also the choices $s = -3n/2$ and $s = -6n$ for which Eq. (29) is quadratic in $\sqrt{y_0}$ and y_0 respectively. However, the solution for y_0 corresponding to these choices is not qualitatively different from that corresponding to $s = 3n$ shown above. The PDL crossing can never take place either.

so that Eq. (29) is linear in y_0. We therefore resort to the choice $s = 3n$ for which Eq. (29) is quadratic in y_0 and the solution for y_0 is given by Eq. (30). Using Eqs. (26), (33) and (30) we obtain

$$y = y_0 + y_1 + y_2 = (\alpha_0 + \alpha_2) a^{-s} + \alpha_1 a^s \pm \alpha_0 a^{-s} \sqrt{1 + \frac{2\alpha_1 a^{2s}}{\alpha_0}}. \qquad (35)$$

For a PDL crossing at $a = a_c$, $y(a = a_c) = 0$, which implies that the parameters α_0, α_1 and α_2 should satisfy the relation

$$\left(\alpha_2 + \alpha_1 a^{2s}\right)^2 + 2\alpha_0 \alpha_2 = 0. \qquad (36)$$

Thus a smooth crossing from a $w_X > -1$ regime to a $w_X < -1$ regime is indeed possible for the choice $s = 3n$, provided one of the parameters α_0 and α_2 must be negative with respect to the other, i.e., $\alpha_0 \alpha_2 < 0$. However, a negative value of α_2 implies an eternally negative definite kinetic energy density ρ_2 for the field ϕ_2. A negative value α_0, on the other hand, does not necessarily imply a negative energy density for the field ϕ_0, which is derived below. We therefore choose to work with $\alpha_0 < 0, \alpha_2 > 0$.

Let us now set $s = 1/2$, so that the DE perturbations are slowly propagating with speed $c_X = \sqrt{n} = 1/\sqrt{6}$, and for which Eq. (20) could be integrated easily. Using Eqs. (19) and (20) one then obtains the expressions for the energy density and pressure components due to the field ϕ_0 as

$$\rho_0 = \frac{6\alpha_0}{7a^{7/2}} \left[1 \pm \left(1 + \frac{4\beta a}{5} + \frac{8\beta^2 a^2}{15}\right) (1 - \beta a)^{3/2}\right] + \lambda_0,$$

$$P_0 = \frac{\alpha_0}{7a^{7/2}} \left[1 \pm \left\{1 + \frac{6\beta a}{5} \left(1 + \frac{4\beta a}{3} + \frac{8\beta^2 a^2}{3}\right)\right\} (1 - \beta a)^{1/2}\right] - \lambda_0, \qquad (37)$$

where λ_0 is a constant and we denote $\beta = -2\alpha_1/\alpha_0$. Using Eqs. (27), (34) and (37) we write the expressions for the total dark energy density $(\rho_X = \rho_0 + \rho_1 + \rho_2)$ and total pressure $(p_X = P_0 + P_1 + P_2)$, for the choice $s = 3n = 1/2$, as

$$\rho_X = \frac{6(\alpha_0 + \alpha_2)}{7a^{7/2}} + \frac{6\alpha_1}{5a^{5/2}} \pm \frac{6\alpha_0}{7a^{7/2}} \left(1 + \frac{4\beta a}{5} + \frac{8\beta^2 a^2}{15}\right) (1 - \beta a)^{3/2} + \lambda,$$

$$p_X = \frac{\alpha_0 + \alpha_2}{7a^{7/2}} - \frac{\alpha_1}{5a^{5/2}} \pm \frac{\alpha_0}{7a^{7/2}} \left[1 + \frac{6\beta a}{5} \left(1 + \frac{4\beta a}{3} + \frac{8\beta^2 a^2}{3}\right)\right] (1 - \beta a)^{1/2} - \lambda, \qquad (38)$$

where $\lambda = \lambda_0 + \lambda_1 + \lambda_2$.

Now, from Eq. (6) we express the normalized Hubble rate $(\tilde{H} = H/H_0)$ as

$$\tilde{H}^2 = \frac{\Omega_{0m}}{a^3} + \frac{6(A_0 + A_2)}{7a^{7/2}} + \frac{6A_1}{5a^{5/2}} \pm \frac{6A_0}{7a^{7/2}} \left(1 + \frac{4\beta a}{5} + \frac{8\beta^2 a^2}{15}\right) (1 - \beta a)^{3/2} + \Lambda, \qquad (39)$$

where $A_0 = \alpha_0/\rho_{0c}, A_1 = \alpha_1/\rho_{0c}, A_2 = \alpha_2/\rho_{0c}, \beta = -2\alpha_1/\alpha_0 = -2A_1/A_0$ and $\Lambda = \lambda/\rho_{0c}$. Eliminating Λ using the condition that at the present epoch $t = t_0$, $a = 1$ and $\tilde{H} = 1$, we obtain

$$\tilde{H}^2 = 1 + \Omega_{0m}\left(a^{-3} - 1\right) + \frac{6(A_0 + A_2)}{7}\left(a^{-7/2} - 1\right) + \frac{6A_1}{5}\left(a^{-5/2} - 1\right)$$

$$\pm \frac{6A_0}{7} \left[a^{-7/2} \left(1 + \frac{4\beta a}{5} + \frac{8\beta^2 a^2}{15}\right) (1 - \beta a)^{3/2} - \left(1 + \frac{4\beta}{5} + \frac{8\beta^2}{15}\right) (1 - \beta)^{3/2}\right]. \qquad (40)$$

One may observe that the parameter β should not be greater than 1 in order that $\tilde{H}^2$ is real, and the model to be valid. Moreover, for positive fractional values of β, for which the PDL crossing could take place, the range of validity of the model is up to a finite time in the future at which the scale factor is $a_{max} = 1/\beta$. Therefore, the lesser the positive fractional value of β, the more the model could be extended to future epochs.

In what follows, we fit this model with the observational data so as to determine the parameters A_0, A_1 and A_2, and finally reconstruct the Lagrangian components $P_0(y_0), P_1(y_1)$ and $P_2(y_2)$ using the best fit values of the parameters.

5. Fitting the model with observational data

We use the most recent SNIa data released by the SN Cosmology Project (SCP) team, viz., the Union data-set [7]. It consists of a total of 414 SN samples analyzed from various sources, reduced to 307 most reliable data points after different outlier rejection cuts and selection tests. These 307 Union data includes large samples of SNIa from the older data-sets by Perlmutter *et al*, Tonry *et al*, Riess *et al*, and others [1, 2, 3, 4], SN Legacy Survey (SNLS) [5], as well as the distant SN observed by the Hubble Space Telescope (HST). The range of data extends up to red-shift $z \sim 1.7$, and the full data can be obtained at http://supernova.lbl.gov/Union.

These data provide the extinction-corrected distance modulus, given by

$$\mu_{obs}(z_i) = m_{obs}(z_i) - M, \tag{41}$$

where m_{obs} is the apparent magnitude of the source SN and M is the absolute magnitude. Theoretically, the apparent magnitude is expressed as

$$m_{th}(z_i) = 5 \log_{10}\left[D_L(z_i)\right] + \bar{M}(M, H_0), \tag{42}$$

where $D_L(z_i)$ is the Hubble free luminosity distance, which for a spatially flat universe is defined in terms of the present matter density parameter Ω_{0m} and the set of theoretical model parameters $\mathbf{A} = (A_0, \ldots, A_{N-1})$ as

$$D_L(z_i) = (1 + z_i) \int_0^{z_i} \frac{d\bar{z}_i}{\tilde{H}(\bar{z}_i; \Omega_{0m}, \mathbf{A})}. \tag{43}$$

$\bar{M}$ is the magnitude zero point offset given by

$$\bar{M}(M, H_0) = M + 5 \log_{10}\left[\frac{H_0^{-1}}{Mpc}\right] + 25 = M - 5 \log_{10} h + 42.38, \tag{44}$$

where h is the Hubble constant H_0 in units of 100 Km s^{-1} Mpc^{-1}.

The theoretical distance modulus $\mu_{th}(z_i)$ is defined by

$$\mu_{th}(z_i) = m_{th}(z_i) - M = 5 \log_{10}\left[D_L(z_i)\right] + \mu_0, \tag{45}$$

where

$$\mu_0 = 42.38 - 5 \log_{10} h, \tag{46}$$

is a nuisance parameter, independent of the data points, and has to be uniformly marginalized over (i.e., integrated out).

The likelihood of Ω_{0m} and the theoretical model parameters $\mathbf{A} = (A_0, \ldots, A_{N-1})$ are determined by minimizing the quantity

$$\chi^2(\mu_0; \Omega_{0m}, \mathbf{A}) = \sum_{i=1}^{N_{tot}} \frac{[\mu_{obs}(z_i) - \mu(z_i)]^2}{\sigma_i^2(z_i)}, \tag{47}$$

where $\sigma_i(z_i), (i = 1, \ldots, N_{tot})$, are the total uncertainties on the data points. For the Union data-set [7] $N_{tot} = 307$.

Now, the marginalization with respect to μ_0 can be done by the following two-step procedure [51]:

1. Expanding χ^2 in terms of μ_0 as

$$\chi^2(\mu_0; \Omega_{0m}, \mathbf{A}) = \tilde{A}(\Omega_{0m}, \mathbf{A}) - 2\mu_0\, \tilde{B}(\Omega_{0m}, \mathbf{A}) + \mu_0^2\, \tilde{C}, \tag{48}$$

where

$$\tilde{A}(\Omega_{0m}, \mathbf{A}) = \sum_{i=1}^{N_{tot}} \frac{[\mu_{obs}(z_i) - \mu(z_i; \mu_0 = 0)]^2}{\sigma_i^2(z_i)},$$

$$\tilde{B}(\Omega_{0m}, \mathbf{A}) = \sum_{i=1}^{N_{tot}} \frac{\mu_{obs}(z_i) - \mu(z_i; \mu_0 = 0)}{\sigma_i^2(z_i)}, \quad \tilde{C} = \sum_{i=1}^{N_{tot}} \frac{1}{\sigma_i^2(z_i)}, \tag{49}$$

one finds that Eq. (48) is minimum for $\mu_0 = \tilde{B}/\tilde{C}$.

2. Substituting this value of μ_0 in Eq. (48) we obtain

$$\tilde{\chi}^2(\Omega_{0m}, \mathbf{A}) \equiv \chi^2\left(\mu_0 = \frac{\tilde{B}}{\tilde{C}}; \Omega_{0m}, \mathbf{A}\right) = \tilde{A}(\Omega_{0m}, \mathbf{A}) - \frac{2}{\tilde{C}}\tilde{B}^2(\Omega_{0m}, \mathbf{A}). \tag{50}$$

Now instead of minimizing χ^2 in Eq. (47), one can minimize $\tilde{\chi}^2$ in Eq. (50) with respect to Ω_{0m} and $\mathbf{A} = (A_0, \ldots, A_{N-1})$, since both the minimized values would be the same.

In the case of the three k-field ($N = 3$) model discussed above, corresponding to the choice $s = 3n = 1/2$, we find good fits to the SNIa data for positive fractional values of $\beta = -2A_1/A_0$, and with the negative sign of square roots appearing in the expression for $\tilde{H}^2$ in Eq. (40). We fit the observational data for two parametric choices of $\beta = 0.5$ and 0.25, for which the model remains valid up to sufficiently large future red-shifts $z = -0.5$ and -0.75 respectively.

$\underline{\beta = 0.5}$: With this choice we get the minimized value of $\chi^2 = 310.411$ for the 307 Union data-set [7], and the best fit values $\Omega_{0m} = 0.26662, A_1 = 1.46422, A_2 = 0.159546$. The minimized χ^2 is better by $\Delta\chi^2 = -2.69$ from that found with the Union data for the two-parameter flat ΛCDM model [7, 8]. The minimized χ^2 per degree of freedom (dof) is also improved by $\Delta(\chi^2/dof) = -0.0019$ from that found in ref. [6] by fitting the flat ΛCDM model with the older SNIa gold data-set [4].

$\underline{\beta = 0.25}$: With this choice we get the minimized $\chi^2 = 310.385$, which is improved further by $\Delta\chi^2 = -0.26$ than that obtained for the previous choice ($\beta = 0.5$). The

best fit values of the present matter density parameter and the model parameters are obtained as: $\Omega_{0m} = 0.26103$, $A_1 = 3.58355$, $A_2 = 0.174564$.
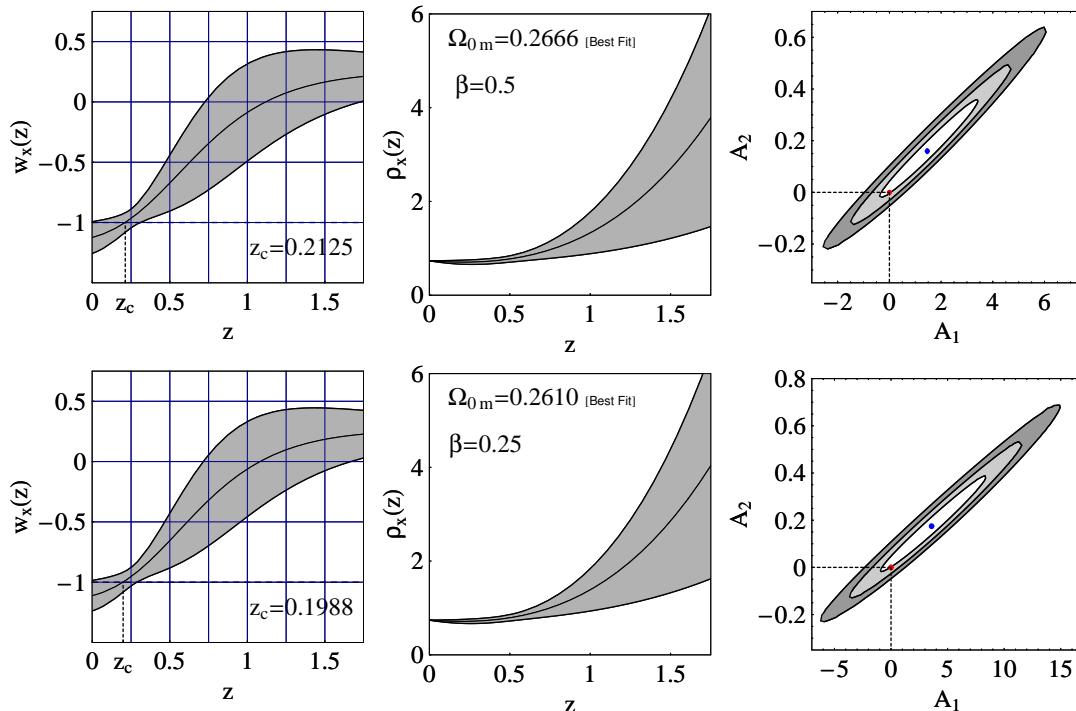
Figure 1. Evolution of $w_X(z)$ and $\rho_X(z)$ (best fit with the Union data, plus 1σ errors) for $0 \leq z \leq 1.75$, as well as the 1σ (white), 2σ (light grey) and 3σ (dark grey) contours in $A_1 - A_2$ parameter space, for the choices $\beta = 0.5$ (upper panels) and $\beta = 0.25$ (lower panels). The point z_c denotes the value of the red-shift at which the PDL ($w_X = -1$) is crossed. The best fit points for both the choices are shown by the dots at the middle of the 1σ $A_1 - A_2$ contours. The cosmological constant, which corresponds to $A_1 = A_2 = 0$, is found to lie on edge of 1σ $A_1 - A_2$ contour for both the choices.

The evolution of $w_X(z)$ and $\rho_X(z)$ (in units of ρ_{0c}), alongwith the corresponding 1σ errors, for $0 \leq z \leq 1.75$, as well as the $1\sigma, 2\sigma$ and 3σ $A_1 - A_2$ contours are shown in Fig. 1, for both the choices $\beta = 0.5$ and 0.25. One may also have the $\Omega_{0m} - A_1$ and $\Omega_{0m} - A_2$ contour plots for either choice, however for brevity we have suppressed those plots. The cases $\beta = 0.5$ and $\beta = 0.25$ are potentially not much distinct. The $w_X(z)$ vs z plots show that the value $z = z_c$ at which the best fit w_X crosses -1 is 0.2125 for $\beta = 0.5$ and 0.1988 for $\beta = 0.25$. Both these values of z_c are fairly in agreement with those obtained for popular model-independent ansatze for $w_X(z)$ [13], $H(z)$ [14], $p_X(z)$ [15], $q(z)$ [16], etc. The cosmological constant (corresponding to $A_1 = A_2 = 0$), is found to be about 1σ away from the best fit result for both the choices $\beta = 0.5$ and $\beta = 0.25$.

The left panel of Fig. 2 shows the variations of the DE EoS parameter $w_X(z)$, the
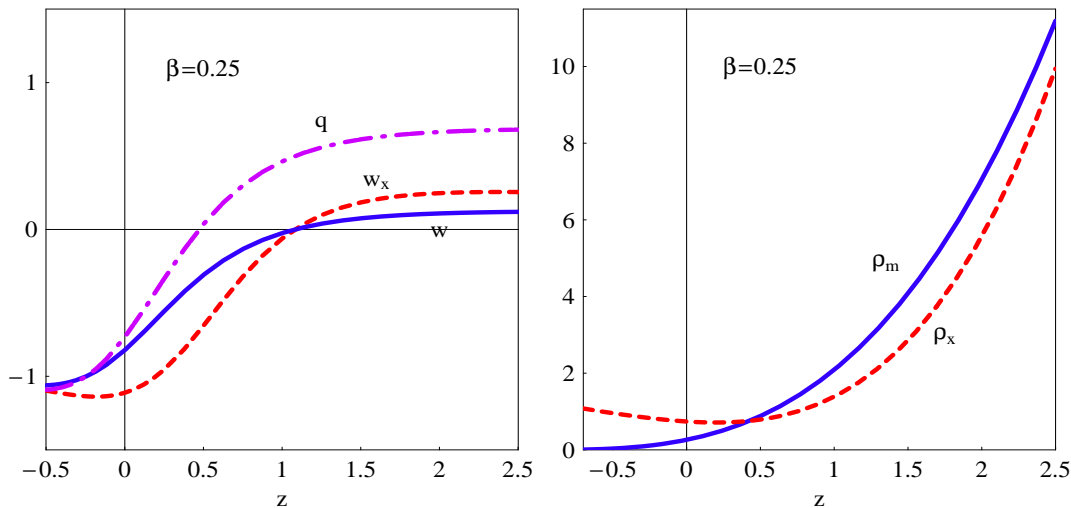
Figure 2. The left panel shows the extrapolations of $w_X(z), w(z)$ and q (best fit with the Union data) to the red-shift range $-0.5 \leq z \leq 2.5$. The DE EoS parameter w_X shows a tendency to back from a minimum value in future towards the cosmological constant value -1. The right panel shows a nearly tracking nature of the dark energy density ρ_X (extrapolated best fit) relative to the matter density ρ_m for high red-shifts $z \gtrsim 1$. Both the plots correspond to the choice $\beta = 0.25$.

total EoS parameter $w(z)$, Eq. (10), and the deceleration parameter $q(z)$, Eq. (11), for the best fit parameters Ω_{0m}, A_1, A_2, extrapolated to the red-shift range $-0.5 \leq z \leq 2.5$. The transition from the decelerating ($q > 0$) phase to the accelerating ($q < 0$) phase occurs at $z \sim 0.45$ and the values of both w and q are greater than -1 at present ($z = 0$). Whereas the present value of $w_X < -1$, there is a tendency that w_X would turn back from a minimum value towards the cosmological constant value ($= -1$) in distant future ($z \lesssim -0.5$). Thus the phantom ($w_X < -1$) phase may be transient, so that future singularities, such as the Big Rip, may be avoided. The right panel of Fig. 2 shows the variations of the matter density ρ_m and the extrapolated best fit DE density ρ_X (both in units of the present critical density ρ_{0c}) with z, for $-0.7 \leq z \leq 2.5$. The DE density is found to almost track the matter density for higher red-shifts, until equalling it at $z \sim 0.4$ and dominant thereafter∥. Thus the model apparently resolves the coincidence problem, side by side providing a PDL crossing DE. The extrapolation of the best fit ρ_X to future epochs also show that the DE density, though dominant, does not run away to very high values, causing Big Rip-like singularities. Both the plots of Fig. 2 correspond to the choice $\beta = 0.25$, for which the model fits better with the

∥ For very high red-shifts ($z \gtrsim 10$) we find that extrapolated ρ_X exceeds ρ_m once again and the DE becomes more and more dominant as we go further and further in the past. However, the best fit model parameters, which give rise to such a variation of $\rho_X(z)$, are found by fitting the Union data available only up to $z \sim 1.7$. Therefore the extrapolation of $\rho_X(z)$ to such high red-shifts, using these parametric values, cannot be trusted with much confidence after all.
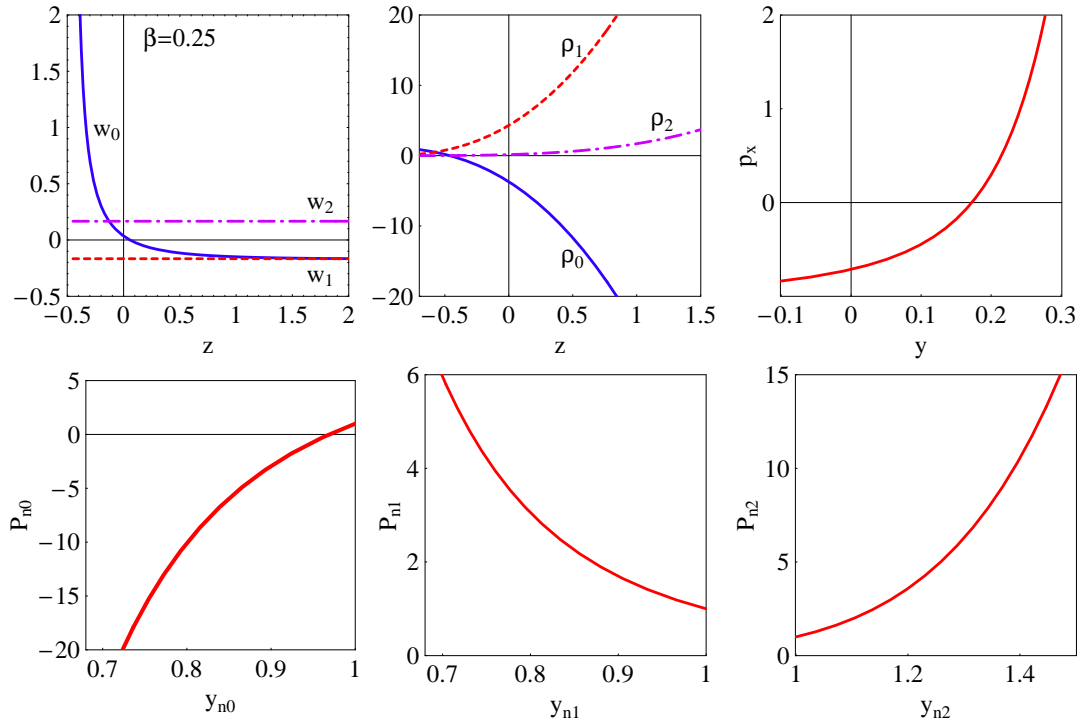
Figure 3. The upper left panel shows the evolution of the individual EoS parameters $w_0(z), w_1(z), w_2(z)$ (extrapolated best fit with the Union data) for $-0.5 \leq z \leq 2$. Whereas w_1 and w_2 are negative and positive constants respectively, w_0 changes from a negative to a positive value in very recent past. The upper middle panel shows the evolution of the individual energy densities $\rho_0(z), \rho_1(z), \rho_2(z)$ (extrapolated best fit with the Union data) for $-0.7 \leq z \leq 1.5$. While ρ_1 and ρ_2 are positive definite, ρ_0 changes from a negative to a positive value at a distant future epoch ($z \approx -0.5$). The upper right panel is a parametric plot (for $0 \leq z \leq 1.75$) showing the variation of the k-essence Lagrangian $p_X = P$ (reconstructed using the best fit model parameters) with $y = y_0 + y_1 + y_2$. The lower panels show the parametric plots (for $0 \leq z \leq 1.75$) of the reconstructed normalized Lagrangian components $P_{n_I} = P_I/P_I^{(0)}$ versus the normalized field gradients $y_{n_I} = y_I/y_I^{(0)}$ for $I = 0, 1, 2$. All the plots correspond to the choice $\beta = 0.25$.

Union data, as mentioned above.

All the plots of Fig. 3 also correspond to the choice $\beta = 0.25$. The upper left panel of Fig. 3 shows the extrapolated best fit variations of the EoS parameters $w_I = P_I/\rho_I$ corresponding to the individual fields ϕ_I ($I = 0, 1, 2$) with red-shift z, for $-0.5 \leq z \leq 2.5$. While $w_1 = -n = -1/6$ and $w_2 = n = 1/6$ are negative and positive constants equal in magnitude, the EoS parameter w_0 increases from a negative constant value (equal to $w_1 = -1/6$) in distant past, crosses zero in very recent past ($z \simeq 0.05$) and then goes on increasing with positive values. The upper middle panel of Fig. 3 shows the extrapolated best fit variations of the individual field energy densities ρ_I with z, for $-0.7 \leq z \leq 1.5$.

ρ_1 and ρ_2 are positive definite and decreases with time (i.e., with decreasing z). ρ_0 is negative in the past and at present, but increases with time, and may become positive in distant future ($z \lesssim -0.5$), as the extrapolations show. In magnitude the value of ρ_2 is found to be very small compared to ρ_0 and ρ_1 for all the red-shift range shown in the figure. ρ_0 and ρ_1, on the other hand, are nearly equal in magnitude for $0 \leq z \leq 0.5$.

Now, the effective DE EoS parameter w_X is given by

$$w_X = \frac{w_0 \rho_0 + w_1 \rho_1 + w_2 \rho_2}{\rho_X} \quad , \qquad \rho_X = \rho_0 + \rho_1 + \rho_2 . \tag{51}$$

Since ρ_X is always positive, the negative definite and positive definite contributors to w_X are ϕ_1 (for which $w_1 < 0, \rho_1 > 0$) and ϕ_2 (for which $w_2 > 0, \rho_2 > 0$) respectively. The field ϕ_0, on the other hand, gives positive contribution ($w_0 \rho_0 > 0$) to w_X right from the past up to $z \simeq 0.05$ and negative contribution ($w_0 \rho_0 < 0$) thereafter. However this field ϕ_0, though has a negative energy density (phantom-like), could not have led to the PDL crossing at $z \simeq 0.2$, as its negative contribution to w_X begins only after $z \simeq 0.05$. It is therefore the (non-phantom-like) field ϕ_1, with positive definite energy density ρ_1, which is effectively responsible for the PDL crossing at $z \simeq 0.2$. This is in contrast with the usual *quintom* mechanism [25] where the negative energy density (phantom) field leads to the PDL crossing at late times. Moreover, none of the three fields above has EoS parameter w_I less than -1, as in quintom models.

We reconstruct the multiple kinetic k-essence Lagrangian $P = p_X$ using the best fit values of the parameters Ω_{0m}, A_1, A_2 for the choice $\beta = 0.25$. The parametric plot of p_X against the total temporal field gradient $y = y_0 + y_1 + y_2$, for red-shifts $z = 0 - 1.75$, in the upper right panel of Fig. 3 shows three separate phases: (i) $p_X > 0$ for $y \gtrsim 0.18$, whence the DE is decelerating ($w_X > 0$), (ii) $-0.7 \lesssim p_X < 0$ for $0 < y \lesssim 0.18$, whence the DE is accelerating but with $w_X > -1$, (iii) $p_X \lesssim -0.7$ for $y < 0$, whence we have a super-accelerating (i.e., phantom-like) DE with $w_X < -1$. The parametric plots of the reconstructed normalized k-essence Lagrangian components $P_{n_I} = P_I / P_I^{(0)}$ (where $P_I^{(0)} = P_I|_{z=0}$, $I = 0, 1, 2$) against the corresponding normalized temporal field gradients $y_{n_I} = y_I / y_I^{(0)}$ (where $y_I^{(0)} = y_I|_{z=0}$, $I = 0, 1, 2$), for $0 \leq z \leq 1.75$, are shown in the lower panels of Fig. 2. In the reconstructions, we have set for simplicity λ_1 and λ_2 appearing in Eqs. (27) and (34) to be zero, whence the cosmological constant term in Eq. (38) is given by $\lambda = \lambda_0$. The pressure P_{n_1} is found to fall off with increasing values of y_{n_1}, whereas the pressures P_{n_0} and P_{n_2} are found to increase, but with opposite rates, with y_{n_0} and y_{n_2} respectively. Since the best fit values of both the parameters A_1, A_2 are positive, the only parameter with a negative value is $A_0 = -2A_1/\beta = -8A_1$ (for $\beta = 0.25$). Therefore, the fields which contribute to the negative part of w_X are ϕ_1 (due to the negative constant value of EoS parameter w_1, but positive definite energy density ρ_1) and ϕ_0 (due to the negative parameter A_0, or α_0, which drives $y_0 = \dot{\phi}_0$ and/or P_0 to be negative, in some regime). However, as explained above, the field ϕ_0 alone is not responsible for the PDL crossing, and it is the field ϕ_1 with Lagrangian component P_1 which effectively causes the super-acceleration ($w_X < -1$).

6. Conclusions

While a PDL crossing DE model involving a single k-essence scalar field suffers from cosmological instabilities [35], a set of multiple k-essence fields are shown to give rise to such PDL crossing, satisfying the conditions for stability even in the simplistic scenario where the k-fields are mutually non-interacting and the individual k-essence Lagrangian densities are purely functions of the kinetic terms. Although there are severe restrictions imposed on the k-field configuration by virtue of the stability criterion, i.e., $c_X^2 \geq 0$, and the non-super-luminescence ($c_X \leq 1$) of the DE density perturbations, we still find certain field configurations for which the DE EoS parameter can cross the cosmological constant barrier. We have worked out the general equation of constraint on the field configuration, with an appropriate choice of the propagation speed, viz., $c_X^2 = a$ constant, lying between 0 and 1. While a configuration of two kinetic k-fields, satisfying the constraint equation, leads to complicated solutions, we have shown that a three k-field configuration gives rise to a cosmologically stable PDL crossing DE model. For certain choices of some of the parameters, the model is found to fit well with the latest SNIa Union data compiled by the Supernova Cosmology Project team [7]. The value of the red-shift $z = z_c$ at which the DE equation of state parameter w_X (best fit with the data) crosses the PDL is found to be $\simeq 0.2$, whereas the best fit present matter density parameter is found to be $\Omega_{0m} \simeq 0.265$. These are in good agreement with the values of z_c and Ω_{0m} found in the likelihood analysis done using other model-dependent or model-independent ansatze in the literature [16, 17, 49]. On the other hand, the value of z at which the universe transits from a decelerating phase to an accelerating phase is found to be ~ 0.65, which also agrees fairly well with other independent studies [16, 17, 49].

In the model which we have presented here, the value of the square of the speed of propagation of the DE density perturbations, c_X^2, is as low as $1/6$ throughout the entire course of the DE evolution. We have worked out the expression for c_X^2 in a general setting of multiple k-essence fields considering the most general scalar type of metric perturbations in a Friedmann-Robertson-Walker background. Although the perturbation equations have been extremely coupled in the curvature and the isocurvature modes, assuming the coupling to be very weak in the sub-Hubble scales the speed of propagation of the curvature perturbations in the multi-k-field case is found to be the one that generalizes the well-known expression for c_X for a single k-essence field found in ref. [45].

The present model exhibits some additional features: Firstly, the dark energy density (best fit with the Union data) almost tracks the matter density in distant past until exceeding the later at $z \simeq 0.4$, thus providing a possible resolution to the coincidence problem. Secondly, the best fit dark energy density, extrapolated to future epochs, does not run away to very high values leading to Big Rip-like singularities even in distant future. Thirdly, the extrapolated best fit of the dark energy equation of state parameter shows a tendency to turn back from a minimum negative value (< -1) towards the cosmological constant value ($= -1$) in distant future, thus indicating a

transient phantom regime.

We have reconstructed the entire k-essence Lagrangian $P(y_0, y_1, y_2)$, as well as the individual Lagrangian components $P_I(y_I)$ in terms of the corresponding field gradients $y_I = \dot{\phi}_I$, using the values of the model parameters best fitting the observational data. The reconstructed total Lagrangian, P is found to be a smooth function of the total field gradient $y = \sum y_I$, i.e., there are no discontinuities or multi-valuedness in the parametric plot of P versus y for the red-shift range under consideration, $0 \leq z \leq 1.75$. All the individual Lagrangian components P_I as functions of the corresponding y_I also show the same smooth nature. The reconstructed Lagrangian P is therefore substantially better than the double-valued Lagrangian found for a single kinetic k-essence field in ref. [52] using popular parameterizations, such as that due to Alam *et al* [14] or due to Chevallier-Polarski-Linder [13] and with the old SNIa gold data-set [3].

A few problems that may be looked upon in the context of the present model are as follows: (i) Can we find a systematic prescription in order to build a stable PDL crossing multiple kinetic k-essence model, instead of choosing the number of k-fields by hand and implementing the value of c_X^2 arbitrarily? (ii) Can we extend the model to sufficiently higher red-shifts so as to match with the CMB and SDSS data? (iii) Is there a way to ascertain how far the isocurvature modes of the density perturbations affect the model at higher red-shifts? (iv) Can we ascertain the status of the future Big Rip singularities, if any, in the context of multi-k-essence, generically, i.e., by not just resorting to particular models? Or, can we generically ascertain whether the phantom regime would be eternal or transient for multiple k-essence? Research works addressing some of these questions are already in progress [46] and we hope to report on them in near future.

Finally, it should be mentioned that although we have not specifically looked to construct tracking/scaling dark energy models in the present paper, the possible avoidance of the coincidence problem in our multi-k-essence model is particularly noteworthy. The value of c_X remains constant and less than the speed of light, unlike in the coincidence resolving single field k-essence models, which are shown to be affected by the super-luminal propagation ($c_X > 1$) of the density perturbations [47]. However, whether our purely kinetic model specifically belongs to the class of tracking or scaling k-essence dark energy, is an interesting issue which we hope to circumvent in future. Assisted accelerated solutions are shown to exist generically for the multi-field k-essence models that have scaling solutions [53]. The nature of such assisted acceleration may also be of some interest for the purely kinetic multi-k-essence, that we have studied here, and is worth investigating.

Appendix: Speed of propagation of multiple k-essence cosmological perturbations

Let us consider the system of N mutually non-interacting k-essence fields coupled to gravity. The gravitational field equations for such a system are

$$G_{\mu\nu} = \kappa^2 T_{\mu\nu} \quad, \qquad T_{\mu\nu} = \sum_{I=0}^{N-1} T_{\mu\nu}^I \,, \tag{52}$$

where $T_{\mu\nu}^I, (I = 0, \ldots, N-1)$ are the energy-momentum tensor components due to the individual k-fields $\mathbf{\Phi} = (\phi_0, \cdots, \phi_{N-1})$, with kinetic terms $\mathbf{X} = (X_0, \cdots, X_{N-1})$, where $X_I = -\frac{1}{2} g^{\mu\nu} \partial_\mu \phi_I \partial_\nu \phi_I$.

The line element with the most general scalar type of perturbations, in an arbitrary gauge, is given by [54]:

$$ds^2 = - \left[1 + 2A(x^i, t)\right] dt^2 + 2a(t)\, \partial_i B(x^i, t)\, dx^i dt$$
$$+ a^2(t) \left[\left(1 + 2\psi(x^i, t)\right) \delta_{ij} + \nabla_j \partial_i E(x^i, t)\right] dx^i dx^j \,, \tag{53}$$

where $a(t)$ is the cosmological scale factor, and $A(x^i, t), B(x^i, t), \psi(x^i, t)$ and $E(x^i, t)$ are the perturbed order variables. The perturbed energy-momentum tensor components are given by

$$T_0^0 = -\left(\bar{\rho} + \delta\rho\right), \quad T_i^0 = -\frac{a}{k}\left(\rho + p\right) \partial_i v \,,$$

$$T_i^j = \left(\bar{p} + \delta p\right) \delta_i^j + \frac{1}{k^2}\left(\nabla_i \nabla^j + \frac{1}{3}\delta_i^j\right)\pi \,, \tag{54}$$

where $\bar{\rho}$ and $\bar{p}$ are the total background energy density and isotropic pressure respectively, $\rho = \bar{\rho} + \delta\rho$ and $p = \bar{p} + \delta p$ are the perturbed total energy density and isotropic pressure respectively, v is the velocity (or, flux) related variable, π is the anisotropic stress, and k is the co-moving wave-number. Decomposing into the components due to individual k-fields, we have

$$\bar{\rho} = \sum_I \bar{\rho}_I \quad, \quad \bar{p} = \sum_I \bar{P}_I \quad, \quad \delta\rho = \sum_I \delta\rho_I \quad, \quad \delta p = \sum_I \delta P_I \quad,$$

$$\rho = \sum_I \rho_I \quad, \quad p = \sum_I P_I \quad, \quad (\rho + p)\, v = \sum_I (\rho_I + P_I)\, v_I \quad, \quad \pi = \sum_I \pi_I \,. \tag{55}$$

The background field equations are the Friedmann equations and the equations of continuity of the individual scalar fields:

$$H^2 \equiv \left(\frac{\dot{a}}{a}\right)^2 = \frac{\kappa^2}{3}\, \rho \,, \tag{56}$$

$$\dot{H} \equiv \frac{\ddot{a}}{a} - \frac{\dot{a}^2}{a^2} = -\frac{\kappa^2}{2}\left(\rho + p\right) \,, \tag{57}$$

$$\dot{\rho}_I + 3H\left(\rho_I + P_I\right) = 0 \quad, \qquad \text{for all } I = 0, \ldots, N-1 \,, \tag{58}$$

The equations for the cosmological perturbations

$$\delta G_\alpha^\beta = \kappa^2 \delta T_\alpha^\beta \,, \tag{59}$$

can be decomposed as

$$H\xi - \frac{k^2}{a^2}\psi = -\frac{\kappa^2}{2}\,\delta\rho \qquad\qquad : \delta G_0^0 \text{ component}\,, \tag{60}$$

$$\xi - \frac{k^2}{a^2}\chi = \frac{3\kappa^2}{2}\frac{a}{k}\,(\rho+p)\,v \qquad\qquad : \delta G_i^0 \text{ component}\,, \tag{61}$$

$$\dot\chi + H\chi = A + \psi \qquad\qquad : \delta G_i^j - \frac{1}{3}\delta_i^j \delta G_k^k \text{ component}\,, \tag{62}$$

$$\dot\xi + 2H\xi + \left(3\dot H - \frac{k^2}{a^2}\right)A = \frac{\kappa^2}{2}\,(\delta\rho + 3\delta p) \qquad : \delta G_k^k - \delta G_0^0 \text{ component}\,, \tag{63}$$

where

$$\chi = a\left(B + a\dot E\right) \quad, \qquad \xi = 3\left(HA - \dot\psi\right) + \frac{k^2}{a^2}\,\chi\,, \tag{64}$$

and note that $\pi = 0$ for a scalar field system in RW background. The quantities ψ, χ and ξ correspond respectively to the three-space curvature, the shear, and the perturbed expansion of the normal-frame vector field [39, 40]. Eq. (60) gives the Arnowitt-Deser-Misner (ADM) energy constraint, Eq. (61) gives the momentum constraint, Eq. (62) is the trace-free part of the ADM propagation, and Eq. (63) is the Raychaudhuri equation [40]. In addition to the above equations, we have the energy and momentum conservation equations given by

$$\delta\dot\rho_I + 3H\left(\delta\rho_I + \delta P_I\right) = \left(\xi - 3HA - \frac{k}{a}v_I\right)(\rho_I + P_I) \quad, \tag{65}$$

$$\frac{\partial_t\left[a^4\left(\rho_I + P_I\right)v_I\right]}{a^4\left(\rho_I + P_I\right)} = \frac{k}{a}\left(A + \frac{\delta P_I}{\rho_I + P_I}\right)\,. \tag{66}$$

The entropic perturbations are given by

$$e_I = \delta P_I - c_I^2 \delta\rho_I \quad, \qquad e = \delta p - c_s^2 \delta\rho\,, \tag{67}$$

where $c_I^2 = \dot P_I/\dot\rho_I$ and $c_s^2 = \dot p/\dot\rho$.

Under a coordinate transformation

$$x^\alpha \to x^\alpha + q^\alpha \quad, \qquad q^\alpha = \left(q^0, q^i\right) \quad; \quad q^0 = \delta t \quad, \quad q^i = \delta^{ij}\partial_j\delta x\,, \tag{68}$$

the metric perturbations transform as

$$A \to A - \dot{\delta t} \quad, \quad B \to B - \frac{\delta t}{a} + a\dot{\delta x} \quad, \quad \psi \to \psi - H\delta t \quad, \quad E \to E - \delta x\,, \tag{69}$$

whereas the field perturbations transform as

$$\delta\phi_I \to \delta\phi_I - \dot\phi_I \delta t\,. \tag{70}$$

Since we are always free to choose δt and δx, we can impose two gauge conditions on the functions A, B, ψ, E or $\delta\rho$ or $\partial_i v$. We choose to work in the commonly used longitudinal

gauge in which $B = E = 0$. Then from Eq. (64) $\chi = 0$, whence Eq. (62) gives $A = -\psi$, and the expression for ξ in Eq. (64) reduces to

$$\xi = -3\left(\dot{\psi} + H\psi\right). \tag{71}$$

Curvature Perturbations:

The so-called gauge-invariant co-moving curvature perturbation variable is given by [55]

$$\Phi = \psi - \frac{a}{k}Hv. \tag{72}$$

From Eqs. (60), (61), (67) and (71), one derives the equations for the curvature perturbations as

$$\dot{\psi} + H\psi = -\frac{\kappa^2}{2}\frac{a}{k}\left(\rho + p\right)v, \tag{73}$$

$$\frac{H^2}{(\rho + p)\,a^3}\partial_t\left(\frac{a^3}{H}\,\delta\rho_v\right) = \frac{k^2}{a^2}\Phi, \tag{74}$$

where the gauge invariant variable $\delta\rho_v$ is defined by

$$\delta\rho_v = \delta\rho - \frac{a}{k}\dot{\rho}v = -\frac{1}{c_s^2}\left(\frac{\rho + p}{H}\dot{\Phi} + e\right). \tag{75}$$

Isocurvature Perturbations:

The total entropic perturbation can be decomposed as [40, 41]

$$e = e_r + \sum_I e_I \quad, \quad e_r = \sum_I \left(c_I^2 - c_s^2\right)\delta\rho_I = \frac{1}{2}\sum_{I,J}\frac{(\rho_I + P_I)\,(\rho_J + P_J)}{\rho + p}c_{IJ}^2 S_{IJ}, \tag{76}$$

where $c_{IJ}^2 = c_I^2 - c_J^2$, and the so-called gauge-invariant isocurvature perturbation variable S_{IJ} is defined as

$$S_{IJ} = \frac{\delta\rho_I}{\rho_I + P_I} - \frac{\delta\rho_J}{\rho_J + P_J}. \tag{77}$$

From Eqs. (65), (66) and (67) one obtains the equations for the isocurvature perturbations

$$\dot{S}_{IJ} = -\frac{k}{a}v_{IJ} - 3He_{IJ} \quad, \quad v_{IJ} = v_I - v_J \quad, \quad e_{IJ} = \frac{e_I}{\rho_I + P_I} - \frac{e_J}{\rho_J + P_J} \quad, \tag{78}$$

$$\ddot{S}_{IJ} + 2H\dot{S}_{IJ} - \frac{3H}{2}\left[\bar{c}_{IJ}^2\dot{S}_{IJ} + \sum_K\frac{\rho_K + P_K}{\rho + p}\left(\dot{S}_{IK} + \dot{S}_{JK}\right)\right]$$

$$+ \frac{k^2}{2a^2}\left[\bar{c}_{IJ}^2 S_{IJ} + c_{IJ}^2\sum_K\frac{\rho_K + P_K}{\rho + p}\left(S_{IK} + S_{JK}\right)\right]$$

$$= -3H\dot{e}_{IJ} - 3\left(\dot{H} + 2H^2\right)e_{IJ} + \frac{9H^2}{2}\left[\bar{c}_{IJ}^2 e_{IJ} + c_{IJ}^2\sum_K\frac{\rho_K + P_K}{\rho + p}\left(e_{IK} + e_{JK}\right)\right]$$

$$- \frac{k^2}{a^2}\left(c_{IJ}^2\frac{\delta\rho_v}{\rho + p} + e_{IJ}\right), \tag{79}$$

where $\bar{c}_{IJ}^2 = c_I^2 + c_J^2$.

Eqs. (73), (74) and (78), (79) form an extremely coupled set of differential equations in the curvature and isocurvature modes, very difficult to solve in general for any system of multiple fields. However, leaving aside the isocurvature terms, one may still work out the effective speed of propagation of curvature perturbations in such a system. In fact, in the large scale limit $(k/a \to 0)$, the curvature mode couples very weakly to the isocurvature ones, as is evident from the term $(k^2/a^2)c_{IJ}\delta\rho_v/(\rho+p)$ on the right hand side of Eq. (79). For a detailed discussion on the issue of decoupling of isocurvature and curvature modes in multiple fluid or field systems, see ref. [40].

Now, in the case of mutually non-interacting multiple k-essence scalar fields, we have the expressions for the total energy density and pressure

$$\rho \equiv \rho_X = \sum_{I=0}^{N-1} \rho_I(\phi_I, X_I) = \sum_{I=0}^{N-1} 2\left[X_I\frac{\partial P_I}{\partial X_I} - P_I(\phi_I, X_I)\right] , \tag{80}$$

$$p \equiv p_X = \sum_{I=0}^{N-1} P_I(\phi_I, X_I) . \tag{81}$$

Using the continuity equations for the fields $\mathbf{\Phi} = (\phi_0, \cdots, \phi_{N-1})$, and the fact that $X_I = \dot{\phi}_I^2/2$ in RW background, we obtain the expressions for the perturbed variables $\delta\rho$ and δp as

$$\delta\rho = \sum_{I=0}^{N-1}\delta\rho_I \quad , \qquad \delta\rho_I = \frac{\dot{\rho}_I}{3H\tilde{c}_I^2}\left(3H\tilde{c}_I^2\sigma_I - \dot{\sigma}_I - \psi\right) , \tag{82}$$

$$\delta p = \sum_{I=0}^{N-1}\delta P_I \quad , \qquad \delta P_I = \frac{\dot{\rho}_I}{3H}\left(3Hc_I^2\sigma_I - \dot{\sigma}_I - \psi\right) , \tag{83}$$

where we have defined $\sigma_I = \delta\phi_I/\dot{\phi}_I$ and $\tilde{c}_I^2 = \frac{\partial P_I}{\partial X_I}/\frac{\partial \rho_I}{\partial X_I}$.

The expressions for v_I and v, obtained from the $0-i$ components of the energy-momentum tensors, are given by

$$v_I = \frac{k}{a}\sigma_I \quad , \qquad v = \frac{k}{a\dot{\rho}}\sum_{I=0}^{N-1}\dot{\rho}_I\sigma_I . \tag{84}$$

Defining further $\sigma = \sum\sigma_I$ and $\sigma_{IJ} = \sigma_I - \sigma_J$, we get from Eqs. (72), (73) and (75)

$$\Phi = \psi - \frac{H\sigma}{N} + \mathcal{O}(\sigma_{IJ}) , \tag{85}$$

$$\dot{\psi} + H\psi = \frac{\dot{H}\sigma}{N} + \mathcal{O}(\sigma_{IJ}) , \tag{86}$$

$$\delta\rho_v = \frac{\dot{F}}{3H^2}\sum_{I=0}^{N-1}\frac{\dot{\rho}_I}{\tilde{c}_I^2} + \mathcal{O}(\sigma_{IJ}) , \tag{87}$$

where N is the total number of fields and for the reasons mentioned earlier we have left aside the terms depending only on σ_{IJ} (and/or its time derivatives), which give rise to the isocurvature modes.

The equation (73) for the curvature mode can now be expressed as

$$\frac{H^2}{(\rho_X + p_X) a^3} \partial_t \left[\frac{(\rho_X + p_X) a^3}{c_X^2 H^2} \dot{\Phi} \right] + \frac{k^2}{a^2} \Phi = \mathcal{O}(\sigma_{IJ}) \quad , \tag{88}$$

where

$$c_X^2 = \dot{\rho} \left[\sum_{I=0}^{N-1} \frac{\dot{\rho}_I}{\tilde{c}_I^2} \right]^{-1} = (\rho_X + p_X) \left[\sum_{I=0}^{N-1} \frac{\rho_I + P_I}{\tilde{c}_I^2} \right]^{-1} , \tag{89}$$

is the effective speed of propagation of the curvature mode of scalar perturbations [46]. For a single k-field ($N = 1, I = 0$), Eq. (89) reduces to the well-known result $c_X^2 = \tilde{c}_0^2 = \partial P_0 / \partial X_0$ [45], whereas for purely kinetic multiple k-essence fields, we have $\tilde{c}_I^2 = c_I^2 = \dot{P}_I / \dot{\rho}_I$, whence $c_X^2 = \dot{\rho} / \sum(\dot{\rho}_I^2 / \dot{P}_I)$. If any of the fields is non-propagating, i.e., $c_I^2 = 0$ for some value of I, then $c_X^2 = 0$.

Under the transformation

$$u = \zeta \Phi \quad , \qquad \zeta = \frac{a\sqrt{\rho_X + p_X}}{c_X H} . \tag{90}$$

the above equation (88) reduces to the familiar form [45, 39, 54, 55]

$$u'' + \left(c_X^2 k^2 - \frac{\zeta'}{\zeta} \right) u = \mathcal{O}(\sigma_{IJ}) \quad , \tag{91}$$

where the prime $\{'\}$ here denotes differentiation with respect to the conformal time η ($= \int dt/a(t)$).

References

[1] S. J. Perlmutter *et al*, Bull. Am. Astron. Soc. **29** 1351 (1997); A. G. Riess *et al*, Astron. J. **116** 1009 (1998); S. J. Perlmutter *et al*, Astrphys. J. **517** 565 (1999).

[2] J. L. Tonry *et al*, Astrophys. J. **594** 1 (2003); R. Knop *et al*, Astrophys. J. **598** 102 (2003); B. Baris *et al*, Astrophys. J. **602** 571 (2004).

[3] A. G. Riess *et al*, Astrophys. J. **607** 665 (2004).

[4] A. G. Riess *et al*, Astrophys. J. **659** 98 (2007).

[5] P. Astier *et al*, Astron. Astrophys. **447** 31 (2006).

[6] T. M. Davis *et al*, Astrophys. J. **666** 716 (2007); G. Miknaitis *et al*, Astrophys. J. **666** 674 (2007); W. M. Wood-Vasey *et al*, Astrophys. J. **666** 694 (2007);

[7] M. Kowalski *et al*, arXiv:0804.4142 [astro-ph].

[8] D. Rubin *et al*, arXiv:0807.1108 [astro-ph].

[9] D. N. Spergel *et al*, Astrophys. J. Suppl. **148** 175 (2003); C. L. Bennet *et al*, Astrophys. J. Suppl. **148** 1 (2003).

[10] D. N. Spergel *et al*, Astrophys. J. Suppl. **170** 377 (2007); J. Dunkley *et al* arXiv:0803.0586 [astro-ph]; R. Hill *et al* arXiv:0803.0570 [astro-ph].

[11] M. Tegmark *et al*, Phys. Rev. **D74** 123507 (2006); D. Eisenstein *et al*, Astrophys. J. **633** 560 (2005).

[12] S. M. Carroll, Living Rev. Rel. **4** 1 (2001); T. Padmanabhan, Phys. Rept. **380** 235 (2006), J. M. Cline, arXiv:hep-th/0612129; J. Polchinski, arXiv:hep-th/0603249; L. M. Krauss and R. J. Scherrer, Gen. Rel. Grav. **39** 1545 (2007).

[13] M. Chevallier and D. Polarski, Int. J. Mod. Phys. **D10** 213 (2001); E. V. Linder, Phys. Rev. Lett. **90** 091301 (2003).

[14] U. Alam, V. Sahni, T. D. Saini and A. A. Starobinsky, Mon. Not. Roy. Astron. Soc. **354** 275 (2004).

[15] M. Visser, CLass. Quant. Grav. **21** 2603 (2004); A. A. Sen, Phys. Rev. **D77** 043508 (2008).

[16] Y. G. Gong and A. Wang, Phys. Rev. **D75** 043520 (2007).

[17] C. A. Shapiro and M. S. Turner, Astrophys. J. **649** 563 (2006); H. K. Jassal, J. S. Bagla and T. Padmanabhan, Mon. Not. Roy. Astron.Soc. **356** L11 (2005); T. R. Choudhury and T. Padmanabhan, Astron. Astrophys. **429** 807 (2005); E. V. Linder and D. Huterer, Phys. Rev. **D72** 043509 (2005); C. Wetterich, Phys. Lett. **B594**, 17 (2004); E. V. Linder, arXiv:0708.0024 [astro-ph]; F. C. Carvalho *et al*, Phys. Rev. Lett. **97** 081301 (2006); J. S. Alcaniz and J. A. S. Lima, Phys. Rev. **D72** 063516 (2005); R. G. Cai and A. Wang, JCAP **0503** 002 (2005).

[18] T. Padmanabhan, Gen. Rel. Grav. **40** 529 (2008); E. J. Copeland, M. Sami and S. Tsujikawa, Int. J. Mod. Phys. **D15** 1753 (2006); P. J. E. Peebles and B. Ratra, Rev. Mod. Phys. **75** 559 (2003); V. Sahni and A. A. Starobinsky, Int. J. Mod. Phys. **D9** 373 (2000).

[19] R. R. Caldwell, R. Dave and P. J. Steinhardt, Phys. Rev. Lett **80** 1582 (1998); S. M. Carroll, Phys. Rev. Lett. **81** 3067 (1998); E. J. Copeland, A. R. Liddle and D. Wands, Phys. Rev. **D57** 4686 (1998); P. J. Steinhardt, L. M. Wang and I. Zlatev, Phys. Rev. **D59** 123504 (1999); I. Zlatev, L. M. Wang and P. J. Steinhardt, Phys. Rev. Lett. **82** 896 (1999); A. R. Liddle and R. J. Scherrer, Phys. Rev. **D59** 023509 (1999).

[20] R. R. Caldwell, Phys. Lett. **B545** 23 (2002); N. Arkani-Hamed, P. Creminelli, S. Mukohyama and M. Zaldarriaga, JCAP **0404** 001 (2004); F. Piazza and S. Tsujikawa, JCAP **0407** 004 (2004); L. P. Chimento and R. Lazkoz, Phys. Rev. Lett. **91** 211301 (2003); S. Tsujikawa, Class. Quant. Grav. **20** 1991 (2003); L. Perivolaropoulos, Phys. Rev. **D71** 063503 (2005); S. Nesseris and L. Perivolaropoulos, Phys. Rev. **D70** 123529 (2004).

[21] S. M. Carroll, M. Hoffman and M. Trodden, Phys. Rev. **D68** 023509 (2003).

[22] J. M. Cline, S. Y. Jeon and G. D. Moore, Phys. Rev. **D70** 043543 (2004).

[23] R. R. Caldwell, M. Kamionkowski and N. N. Weinberg, Phys. Rev. Lett. **91** 071301 (2003).

[24] S. Nojiri, S. D. Odintsov and S. Tsujikawa, Phys. Rev. **D71** 063004 (2005).

[25] B. Feng, X. L. Wang and X. M Zhang, Phys. Lett. **B607** 35 (2005); Z. K. Guo, Y. S. Piao, X. M. Zhang and Y. Z. Zhang, Phys. Lett. **B608** 177 (2005); B. Feng, M. Li, Y. S. Piao and X. Zhang, Phys. Lett. **B634** 101 (2006); R. Lazkoz and G. Leon, Phys. Lett. **B638** 303 (2006); R. Lazkoz, G. Leon and I. Quiros, Phys. Lett. **B649** 103 (2007); Y. Cai, M. Li, J. X. Lu, Y. S. Piao, T. Qiu and X. Zhang, Phys. Lett. **B651** 1 (2007); Y. Cai, H. Li, Y. S. Piao, X. Zhang, Phys. Lett. **B646** 141 (2007).

[26] B. Boisseau, G. Esposito-Farese, D. Polarski and A. A. Starobinsky, Phys. Rev. Lett. **85** 2236 (2000); G. Esposito-Farese and D. Polarski, Phys. Rev. **D63** 063504 (2001); L. Perivolaropoulos, JCAP **0510** 001 (2005); S. Nesseris and L. Perivolaropoulos, Phys. Rev. **D73** 103511 (2006).

[27] V. Sahni and Y. Shtanov, JCAP **0311** 014 (2003); V. Sahni and Y. Shtanov, Phys. Rev. **D71** 084018 (2005).

[28] N. Arkani-Hamed, P. Creminelli, S. Mukohyama and M. Zaldariagga, JCAP **0404** 001 (2004); F. Piazza and S. Tsujikawa, JCAP **0407** 004 (2004).

[29] V. K. Onemli and R. P. Woodard, Class. Quant. Grav. **19** 4607 (2002); V. K. Onemli and R. P. Woodard, Phys. Rev. **D70** 107301 (2004); E. O. Kahya and V. K. Onemli, Phys. Rev. **D76** 043512 (2007).

[30] B. Gumjudpai, T. Naskar, M. Sami and S. Tsujikawa, JCAP **0506** 007 (2005).

[31] See for example, L. Amendola and S. Tsujikawa, Phys. Lett. **B660** 125 (2008); and references therein.

[32] H. Wei, R. G. Cai and D. F. Zeng, Class. Quant. Grav. **22** 3189 (2005); H. Wei and R. G. Cai, Phys. Rev. **D72** 123507 (2005); H. Wei, N. N. Tang and S. N. Zhang, Phys. Rev. **D75** 043009 (2007).

[33] C. Armendariz-Picon, V. F. Mukhanov and P. J. Steinhardt, Phys. Rev. Lett. **85** 4438 (2000); C. Armendariz-Picon, V. F. Mukhanov and P. J. Steinhardt, Phys. Rev. **D63** 103510 (2001); C.

Armendariz-Picon, T. Damour and V. F. Mukhanov, Phys. Lett. **B458** 209 (1999); T. Chiba, T. Okabe and M. Yamaguchi, Phys. Rev. **D62** 023511 (2000).

[34] M. Malquarti, E. J. Copeland, A. R. Liddle and M. Trodden, Phys. Rev. **D67** 123503 (2003); M. Malquarti, E. J. Copeland and A. R. Liddle, Phys. Rev. **D68** 023512 (2003); J. M. Aguirregabiria, L. P. Chimento and R. Lazkoz, Phys. Rev. **D70** 023509 (2004); L. P. Chimento and A. Feinstein, Mod. Phys. Lett. **A19** 761 (2004); L. P. Chimento, Phys. Rev. **D69** 123517 (2004).

[35] A. Vikman, Phys. Rev. **D71** 023515 (2005).

[36] S. Capozziello, S. Nojiri and S. D. Odintsov, Phys. Lett. **B632** 597 (2006); S. Nojiri and S. D. Odintsov, Gen. Rel. Grav. **38** 1285 (2006).

[37] A. A. Andrianov, F. Cannata and A. Y. Kamenshchik, Phys. Rev. **D72** 043531 (2005); F. Cannata and A. Y. Kamenshchik, Int. J. Mod. Phys. **D16** 1683 (2007); A. K. Sanyal, arXiv:0710.3486 [astro-ph].

[38] L. P. Chimento and R. Lazkoz, Phys. Lett. **B639** 591 (2006).

[39] J. Hwang, Astrophys. J. **375** 443 (1991).

[40] J. Hwang and H. Noh, Class. Quant. Grav. **19** 527 (2002); J. Hwang and H. Noh, Phys. Lett. **B495** 277 (2000).

[41] H. Kodama and M. Sasaki, Prog. Theor. Phys. Suppl. **78** 1 (1984); H. Kodama and M. Sasaki, Int. J. Mod. Phys. **A1** 265 (1986); *ibid* **A2** 491 (1987).

[42] C. Gordon, D. Wands, B. A. Bassett and R. Maartens, Phys. Rev. **D63** 023506 (2001).

[43] D. Langlois and S. Renaux-Petel, JCAP **0804** 017 (2008); D. Langlois, S. Renaux-Petel, D. A. Steer and T. Tanaka, 0806.0336 [hep-th]; X. Gao, JCAP **0806** 029 (2008).

[44] F. Arroja, S. Mizuno and K. Koyama, JCAP **0808** 015 (2008); D. Langlois, S. Renaux-Petel, D. A. Steer and T. Tanaka, Phys. Rev. Lett. **101** 061301 (2008); M. Huang, G. Shiu and B. Underwood, Phys. Rev. **D77** 023511 (2008); D. A. Easson, R. Gregory, D. F. Mota, G. Tasinato and I. Zavala, JCAP **0802** 010 (2008).

[45] J. Garriga and V. F. Mukhanov, Phys. Lett. **B458** 219 (1999).

[46] S. Sur, *in preparation*.

[47] C. Bonvin, C. Caprini and R. Durrer, Phys. Rev. Lett. **97** 081303 (2006) [arXiv:astro-ph/0606584].

[48] E. Babichev, V. F. Mukhanov and A. Vikman, JHEP **0802** 101 (2008); E. Babichev, V. F. Mukhanov and A. Vikman, JHEP **0609** 061 (2006); J. Bruneton, Phys. Rev. **D75** 085013 (2007); J. Bruneton and G. Esposito-Farese, Phys. Rev. **D76** 124012 (2007).

[49] S. Nesseris and L. Perivolaropoulos, JCAP **0701** 018 (2007); S. Nesseris and L. Perivolaropoulos, Phys. Rev. **D72** 123519 (2005); V. Sahni and A. A. Starobinsky, Int. J. Mod. Phys. **D15** 2105 (2006); U. Alam, V. Sahni and A. A. Starobinsky, JCAP **0702** 011 (2007); L. P. Chimento, R. Lazkoz, R. Maartens and I. Quiros, JCAP **0609** 004 (2006); S. Fay and R. Tavakol, arXiv:0801.2128 [astro-ph].

[50] S. Sur and S. Das, *in preparation*.

[51] L. Perivolaropoulos, Phys. Rev. **D71** 063503 (2005); E. Di Pietro and J. F. Claeskens, Mon. Not. Roy. Astron.Soc. **341** 1299 (2003).

[52] A. A. Sen, JCAP **0603** 010 (2006).

[53] S. Tsujikawa, Phys. Rev. **D73** 103504 (2006) [arXiv:hep-th/0601178].

[54] J. M. Bardeen, Phys. Rev. **D22** 1882 (1980); V. F. Mukhanov, H. A. Feldman and R. H. Brandenberger, Phys. Rept. **215** 203 (1992); V. F. Mukhanov, *Physical Foundations of Cosmology*, Cambridge Univ. Press, Cambridge, UK (2005).

[55] J. Hwang and E. T. Vishniac, Astrophys. J. **353** 1 (1990); G. V. Chibisov and V. F. Mukhanov, Mon. Not. Roy. Astron. Soc. **200** 535 (1982); V. N. Lukash, Sov. Phys. - JETP Lett. **31** 596 (1980); V. N. Lukash, Sov. Phys. - JETP **52** 807 (1980).